Int. J Heat Mass Transfer Vol 20, pp 159–169 Pergamon Press 1977 Printed in Great Britain

FLOW STUDIES FOR NATURAL CONVECTION IN LIQUIDS BETWEEN A SPHERE AND ITS CUBICAL ENCLOSURE

RALPH E. POWE,* JACK A. SCANLAN† and THOMAS A. LARSON‡

(*Received* 20 *January* 1976 *and in revised form* 2 *June* 1976)

Abstract—The results of a flow visualization study of natural convection in liquids contained between a heated sphere and its cooled cubical enclosure are reported in this paper. Three different spheres were utilized in conjunction with a cube 25.15 cm on a side to obtain dimension ratios (ratio of cube edge length to sphere diameter) ranging from 1.10 to 2.20 and Grashof numbers from 0.5 to 50 000 000. Detailed descriptions of the flow patterns are presented, and these descriptions are substantiated by photographs of the flow. Fluids utilized include water, 20 cSt silicone oil, and 350 cSt silicone oil. It was possible to categorize the flow patterns for all of these fluids and geometries into four steady patterns and four unsteady patterns. Except for the smallest dimension ratio, 1.10, steady flows always occurred at small Grashof numbers, while unsteady flows occurred for large Grashof numbers. Interference between up-flow and down-flow layers was noted for the smallest dimension ratio, and this created a rather unique flow pattern.

NOMENCLATURE

- D, sphere diameter;
- g, gravitational acceleration;
- Gr, Grashof number, $g\beta\rho^2L^3\Delta T/\mu^2$;
- L, characteristic dimension, $(S-D)/2$;
- R, dimension ratio, S/D;
- S, edge length of cube;
- T_i, sphere surface temperature;
- T_0, cube surface temperature;
- ΔT, temperature difference between sphere and cube, T_i-T_0;
- β, thermal expansion coefficient;
- ρ, fluid density;
- μ, fluid viscosity.

INTRODUCTION

HEAT transfer by natural convection from a body to its finite enclosure is of importance in nuclear reactor technology, electronic instrumentation packaging, aircraft cabin design, the analysis of fluid suspension gyrocompasses, and numerous other practical situations. Accurate prediction of such heat-transfer rates, which can now only be roughly approximated, is required in many engineering design problems. Since natural convection flow fields are buoyancy driven due to thermal effects, the thermal fields and hydrodynamic fields are very closely coupled, and a knowledge of the flow field is essential to the complete understanding of the heat-transfer phenomena. Also, the unusual stability conditions associated with this problem are of fundamental interest in the fields of heat transfer and fluid mechanics.

From an analytical standpoint the problem of natural convection in enclosed spaces is complicated by the fact that boundary-layer approximations and simplifying assumptions regarding pressure gradients normally made in the analysis of simple bodies in an infinite atmosphere are not valid for enclosed spaces. As a result, analytical solutions have been developed only for the simplest geometries, concentric cylinders [1, 2] and concentric spheres [3], and even these solutions are valid only for small values of the Grashof number. Numerical integration of the governing equations for steady laminar flow between concentric cylinders was presented by Crawford and Lemlich [4], Abbott [5], and Powe *et al.* [6], but these solutions are still generally valid only for low Grashof numbers since the flow becomes unsteady for large values of the Grashof number. Also, computational time is generally excessive.

Experimental studies of both the heat-transfer problem and the flow problem have previously been conducted for the relatively simple concentric sphere [7–9] and concentric cylinder [10–13] geometries, and heat-transfer studies have recently been extended to include more complicated configurations with a spherical outer body [14, 15]. Both the concentric sphere and the concentric cylinder flow studies indicated that for small Grashof numbers the flow was of a steady nature. For Grashof numbers above some transition value the flow was unsteady, and the characteristics of the unsteadiness were highly dependent upon the geometry. However, the unsteadiness was found to always appear first in the extreme upper portion of the flow field.

The purpose of the present paper is to present flow visualization results for natural convection in a somewhat more complicated geometry than has been studied in the past. This geometry consists of the space between a sphere and its cubical shaped enclosure. The geometric centers of the sphere and the cube are coincident.

* Associate Professor, Mechanical Engineering Department, Mississippi State University, Mississippi 39762, U.S.A.

† Professor, Mechanical Engineering Department, Montana State University.

‡ Graduate Research Assistant, Mechanical Engineering Department, Montana State University.

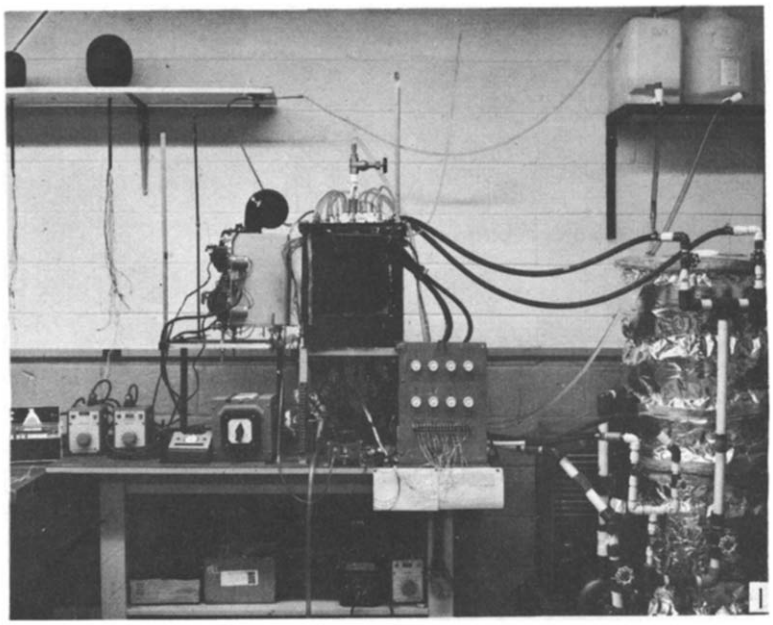

FIG. 1. Flow visualization apparatus.

Water, 20 cSt silicone oil, and 350 cSt silicone oil were used as test fluids in this geometry. Detailed descriptions of the flow patterns which occurred are presented, and these descriptions are supported by actual flow photographs.

APPARATUS AND PROCEDURE

The flow visualization apparatus shown in Fig. 1 consists of a sphere mounted concentrically within a cubical body. This entire assembly was mounted within a cubical enclosure. Values of the dimension ratio of 2.20, 1.41, and 1.10 were obtained by utilizing inner spheres of 11.43, 17.78 and 22.86 cm O.D. in conjunction with a single outer cube 25.15 cm on an inside edge. The inner spheres were 0.076-cm thick copper, and the outer cube was 0.65 cm thick plexiglass.

The inner spheres, which were painted flat black to minimize reflections, were supported in the outer cube by a 0.13-cm dia stainless steel stem which was insulated on its lateral surface. The inner body surface temperature was kept uniform by a heating tape arrangement. Adhesive metallic tapes, 0.051-cm thick and 0.320 cm in width, were affixed to the inner surface of these bodies. These tapes consisted of a resistance wire embedded in a metallic insulative foil on one surface and an adhesive compound on the other surface. To insure that the tapes remained in place, after installing the tapes, a thin layer of silicone sealant was applied over the entire surface, and the bodies were filled with a loose insulating material before being used. As many as eight different tape segments were utilized in each body, and the power input to each of the segments could be individually adjusted to obtain an isothermal inner body surface. Surface temperatures were monitored by a number of thermocouples mounted flush with the outside surface, and thermocouple leads exited via the inner body support stem.

In order to meet transparency requirements, the outer body was made of 0.64-cm plexiglass. All edges were fastened by screws, while a silicone sealant was used during assembly to insure a leak-proof container. All surfaces, except for two mutually perpendicular sides and the top, were painted flat black to minimize light reflections. The surface temperature of the cube was monitored by 21 thermocouples placed over the entire surface. These were mounted flush with the inner surface of the cube, through small holes drilled in the plexiglass, and were epoxied in place.

Surrounding the outer body was a cubical enclosure through which cooling water could be circulated. The top and two mutually perpendicular side faces were made of 1.27-cm thick sheet plexiglass, and the bottom and the other two sides were made of sheet aluminum. To permit changing of the spheres, the enclosure was designed so that the top cover could be easily removed. In order to minimize optical reflections, the inner surfaces of the cubical enclosure were lined with thin phenolic sheets painted flat black with the exception of the viewing port and a 0.50-cm wide vertical lighting slit.

In order to maintain the outer cube in an isothermal condition, a forced water flow was provided by a centrifugal pump to the enclosure, which served as a water jacket. The water jacket was equipped with individual channels so that cooling water could be circulated independently over the four sides, the top, and the bottom of the cubical test space. The water chilling and circulating system was constructed so that that coolant flow rate in each channel could be controlled independently. It was found that this

arrangement enabled the outer cube to be maintained in an isothermal condition.

The inner sphere support stem passed through the outer plexiglass cube and the cubical enclosure through O-ring seals and was connected to a small cylindrical stainless steel reservoir. The reservoir provided means of connecting electrical leads to the heaters and leads to the inner sphere surface thermocouples. The reservoir rested on a threaded rod which was used to position the sphere along the vertical axis of the outer cube.

A thin collimated plane of light from three 300W quartz iodine high intensity lamps passed through the flow field. After injection of the test fluid containing tracer particles into the gap, these permitted visual and photographic observation of the flow in a plane by viewing at right angles to the collimated light beam.

The procedure used in visualizing a flow pattern was as follows. First, the test fluid containing tracer particles was introduced into the gap. For water as the test fluid tracer particles were obtained from a detergent using the technique described by Powe *et al.* [16]. With the silicone oils, a flourescent paint was sprayed on an open surface of the fluid, and the paint was allowed to diffuse through the oil.

After the test fluid had been introduced into the gap the flow of cooling water was initiated, and the temperature of the outer cube was allowed to come to equilibrium. The power inputs to the heating tapes were adjusted to obtain an isothermal inner body surface with the desired temperature difference between inner and outer bodies. After the flow pattern had stabilized, still photographs were obtained using a tripod mounted 4×5-in Calumet camera, and moving pictures were recorded with a Beaulieu R16 movie camera and Kodak 4X reversal film. Kodak Tri-XPan professional film or Polaroid black and white 3000 speed land film was used for all still photographs, and Kodabromide F.4 print paper was used for enlargement and printing to achieve good contrast.

For each observation the temperatures of the inner and outer bodies were recorded. A Grashof number was then defined in the following manner:

$$Gr = g\beta\rho^2 L^3 \Delta T/\mu^2, \tag{1}$$

where L is the characteristic dimension taken as one half the difference between the edge length of the cube and the sphere diameter. All fluid properties are based on the arithmetic mean temperature of the two surfaces, and the geometry is characterized by a dimension ratio,

$$R = S/D. \tag{2}$$

DISCUSSION OF RESULTS

As has previously been observed for concentric cylinders and concentric spheres, it was found in the current investigation that a steady flow pattern occurred at low Grashof numbers, while an unsteady pattern occurred for Grashof numbers above some transition value. For all the fluids investigated, it was possible to classify the steady flows into four different categories, all of which are modifications of a basic pattern, termed a peripheral flow pattern. The unsteady flow patterns were divided into four basically different classifications. These general trends were followed for all dimension ratios studied except the smallest, 1.10; thus, the flows for this dimension ratio will be discussed separately.

For all the liquids investigated, the basic steady flow pattern observed at low Grashof numbers is termed a peripheral flow pattern. Figure 2 illustrates this type of flow for the dimension ratio of 1.41 with 350 cSt silicone fluid. A high-speed fluid layer basically follows the solid boundaries of the system. The fluid in this layer proceeds over the surface of the inner body and separates at a point near the upper vertical axis of the sphere forming a thermal plume around the axis. The fluid then moves across the top and down the side of the cubical enclosure. In some instances, a definite point of separation of this down-flow layer from the vertical cube surface was observed, although this is not the case in Fig. 2. Here, over a significant length along the vertical cube surface, a small amount of fluid leaves the primary flow and gradually migrates toward the inner body. When a point of separation did occur, the region below the point of separation was filled with essentially stagnant fluid. This pattern was symmetrical about the vertical axis in the plane of observation.

In some instances the flow at low Grashof numbers consisted of the peripheral flow pattern modified by the appearance of an interior secondary cell as illustrated in Fig. 3 for a dimension ratio of 2.20 with the silicone 20 cSt fluid. Three fundamental regions in this pattern can be identified: (1) a layer of high-speed fluid which followed the geometric boundary of the system; (2) an upper interior region; and (3) a lower stagnant region. As seen from Fig. 3, the high-speed fluid flowed upward over the surface of the sphere and separated from the sphere surface forming a chimney around the upper vertical axis. Near the top of the cube, a portion of the fluid was turned downward toward the surface of the inner body, giving rise to a pair of vortices, one to either side of the chimney. The portion of fluid that flowed across the top entrained a small amount of fluid from the central region of the flow field and then proceeded down the side of the enclosing cube. At a point on the side of the cube at the same elevation as the bottom of the inner body, a portion of the fluid flowing down the side of the cube separated and slowly moved inward toward the spherical body. The remaining fluid continued down the cube side into the lower stagnant region. The point of separation on the side of the cubical enclosure became more pronounced as the Grashof number was increased. It should be noted that there is a great deal of similarity between this pattern and the basic steady flow pattern reported by Yin *et al.* [9] for water contained between concentric spheres.

For all fluids and dimension ratios investigated, the basic steady flow pattern did not change directly to an unsteady flow pattern as the Grashof number was increased. Instead, a second type of steady flow pattern would be formed for an intermediate range of Grashof numbers. Two such flow patterns were encountered: a peripheral flow with recirculation and a peripheral flow

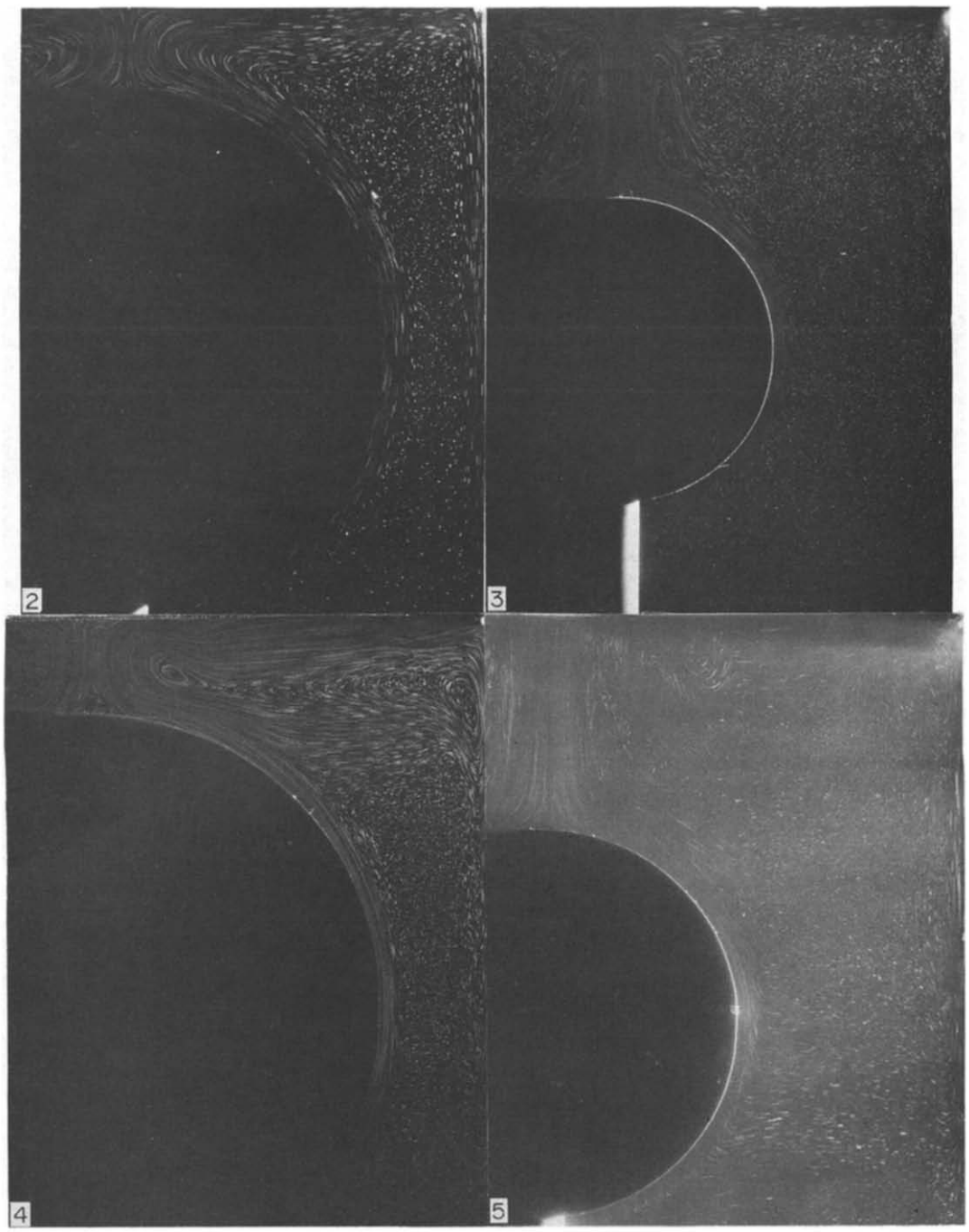

FIG. 2. Peripheral flow pattern for 350 cSt silicone fluid, $R = 1.41$, $Gr = 57$.

FIG 3. Peripheral flow with interior secondary cell for 20 cSt silicone fluid, $R = 2.20$, $Gr = 22\,800$.

FIG. 4. Peripheral flow with recirculation for 20 cSt silicone fluid, $R = 1.41$, $Gr = 32\,000$.

FIG 5. Peripheral flow with interior secondary and tertiary cells for water, $R = 2.20$, $Gr = 2\,649\,000$.

with interior secondary and tertiary cells. In addition, the peripheral flow with an interior secondary cell was observed as an intermediate steady flow pattern in some instances.

In the peripheral flow with recirculation, fluid from the central region of the gap was entrained by the high-speed layer flowing over the surface of the inner body. This resulted in a general movement of some of the fluid from the layer flowing down the side of the cubical enclosure toward the sphere. As a consequence of this recirculation, two large rotating cells were formed in the upper portion of the gap. One of these was adjacent to the chimney, and the other was a corner eddy formed at the upper edge of the cube. The lower portion of the flow field remained similar to the basic peripheral flow pattern. Figure 4 shows a photograph of the recirculation flow for a dimension ratio of 1.41 with the 20 cSt silicone fluid. Evident in Fig. 4 are two very small counter-rotating cells on the surface of the inner body near the base of the chimney. These cells were formed as a small amount of fluid from the boundary flow over the sphere drifted into the vertical axis region near the top of the inner body. The main boundary flow then detoured around this small region in which the fluid moved about randomly. The random motion continued for only a few seconds before formation of the two cells. The formation of these cells was followed by their upward movement until they were absorbed by the boundary flow across the top. A well-developed flow in the chimney region would then form for a short period after which the sequence of events just described would again occur. This process was noted to be repeated with a period of approximately 110 s. The presence of this small region of unsteadiness had no noticeable effect on the remainder of the flow field.

The next steady flow pattern observed was a peripheral flow with interior, secondary and tertiary cells, as illustrated in Fig. 5 for a dimension ratio of 2.20 with water as the test fluid. The flow moves over the surface of the sphere, turns upward at the top of the body to form a thermal plume, and then proceeds across the top and down the side of the enclosure to a region of separation. Three large cells are formed in the upper portion of the gap adjacent to the chimney. A corner eddy at the upper edge of the cube and several small eddies along the side of the cubical enclosure were noted with this pattern. This flow is somewhat similar to the tertiary flow pattern reported by Yin *et al.* [9] for water contained between concentric spheres.

The unsteady flow patterns observed for Grashof numbers above the transition value appeared to be much more dependent on the dimension ratio than on the particular fluid utilized. However, the exact value of the transition Grashof number did depend to some extent on the fluid (i.e. the Prandtl number).

For the dimension ratio of 2.20, with both the 20 cSt silicone and the 350 cSt silicone, the unsteady flow is termed a climbing vortices pattern. The sequence of events associated with this pattern is illustrated in Figs. 6 and 7 for the 350 cSt silicone fluid. Two cells were formed periodically adjacent to the chimney as shown

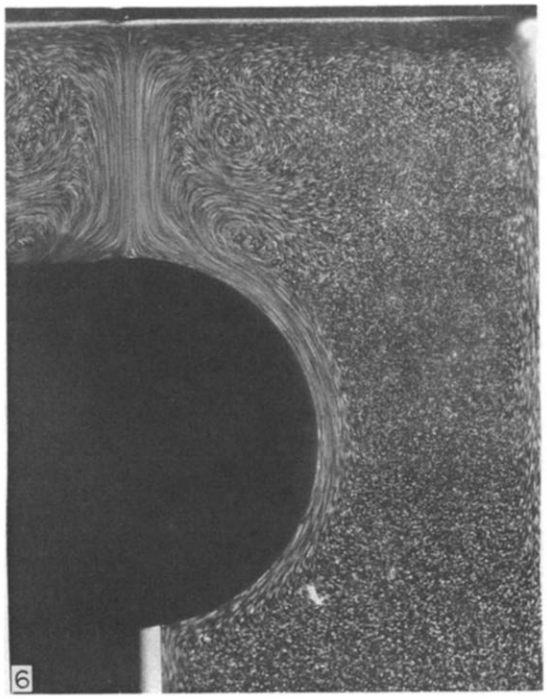

FIG. 6. Steady portion of flow cycle for climbing vortices pattern with 350 cSt silicone fluid, $R = 2.20$, $Gr = 800$.

in Fig. 6. The cells remained stationary for a short time and then proceeded to move upward along the sides of the chimney as shown in Fig. 7. In this process the cells were completely dissipated. Details concerning this pattern for the different fluids will be given later in this discussion.

For water as the test fluid with a dimension ratio of 2.20, the unsteadiness became evident only in the interior portion of the flow field. The high-speed boundary flow remained essentially undisturbed, but the upper central region was dominated by three-dimensional unsteady activity. The interior, secondary and tertiary cells no longer existed. Instead, a three-dimensional cell was formed near the top of the enclosure at non-periodic intervals. This cell would then move out into the interior region, violently disrupting this portion of the gap. Figure 8 indicates this cell and the rather unpredictable activity in the upper interior region.

For all three liquids studied, a random cellular flow was observed to be the unsteady pattern for a dimension ratio of 1.41. Although some of the details of this pattern varied for the different fluids, the major characteristics may be observed in Fig. 9, which is for the 20 cSt silicone fluid. In this pattern, the primary flow over the inner body surface separated from the surface before reaching the upper vertical axis. The resulting space in the upper vertical axis region was generally filled with an erratic cellular flow. As pictured in Fig. 9, recirculation generally occurred in the upper portion of the gap for this flow field, and the tendency toward recirculation became stronger as the Grashof number was increased.

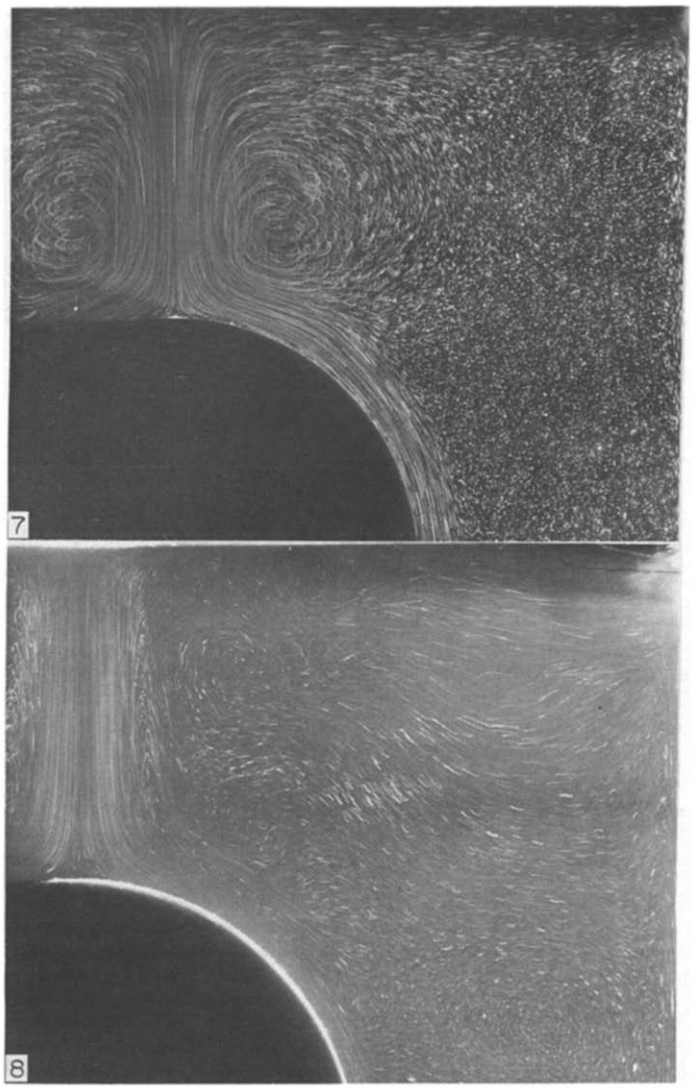

FIG. 7. Unsteady portion of flow cycle for climbing vortices pattern with 350 cSt silicone fluid, $R = 2.20$, $Gr = 800$.

FIG. 8 Unsteady interior flow for water, $R = 2.20$, $Gr = 16\,782\,000$.

The foregoing classifications of steady and unsteady flow patterns incorporate all of the flows observed for all fluids and all dimension ratios, except the smallest investigated, 1.10. For this dimension ratio, the flow was of a completely different type than has been previously observed. It exhibited some unsteady characteristics throughout the range of Grashof numbers considered, regardless of the fluid under test. This pattern is termed a binary flow since it appears to be divided into two separate regions by the close proximity of the inner body and the cube at the mid-plane of the sphere. A typical binary flow pattern is shown in Fig. 10. The division of the flow pattern apparently did not effect the majority of the primary high-speed flow. The upper central region was bounded by the narrow gap at the mid-plane of the sphere, by the flow over the sphere surface, and by the flow over the top and side of the enclosed cube. A similar occurrence was observed in the lower gap region. The upper vertical axis region was dominated by unsteady activity for all cases investigated, and this unsteadiness was generally characterized by the non-periodic formation and dissipation of numerous three-dimensional eddies. An interesting variation of this pattern occurred for the 20 cSt silicone fluid at high Grashof numbers, and this pattern is shown in Fig. 11. In this case, recirculation accompanied by several small eddies occurred in the upper gap region. Also, numerous small eddies appear in the lower central region just below the horizontal mid-plane of the sphere. The flow in this area was strikingly similar to that previously obtained by Elder [17, 18] and Watson [19] for natural convection in a rectangular cavity.

Categorizations of the specific flow patterns which

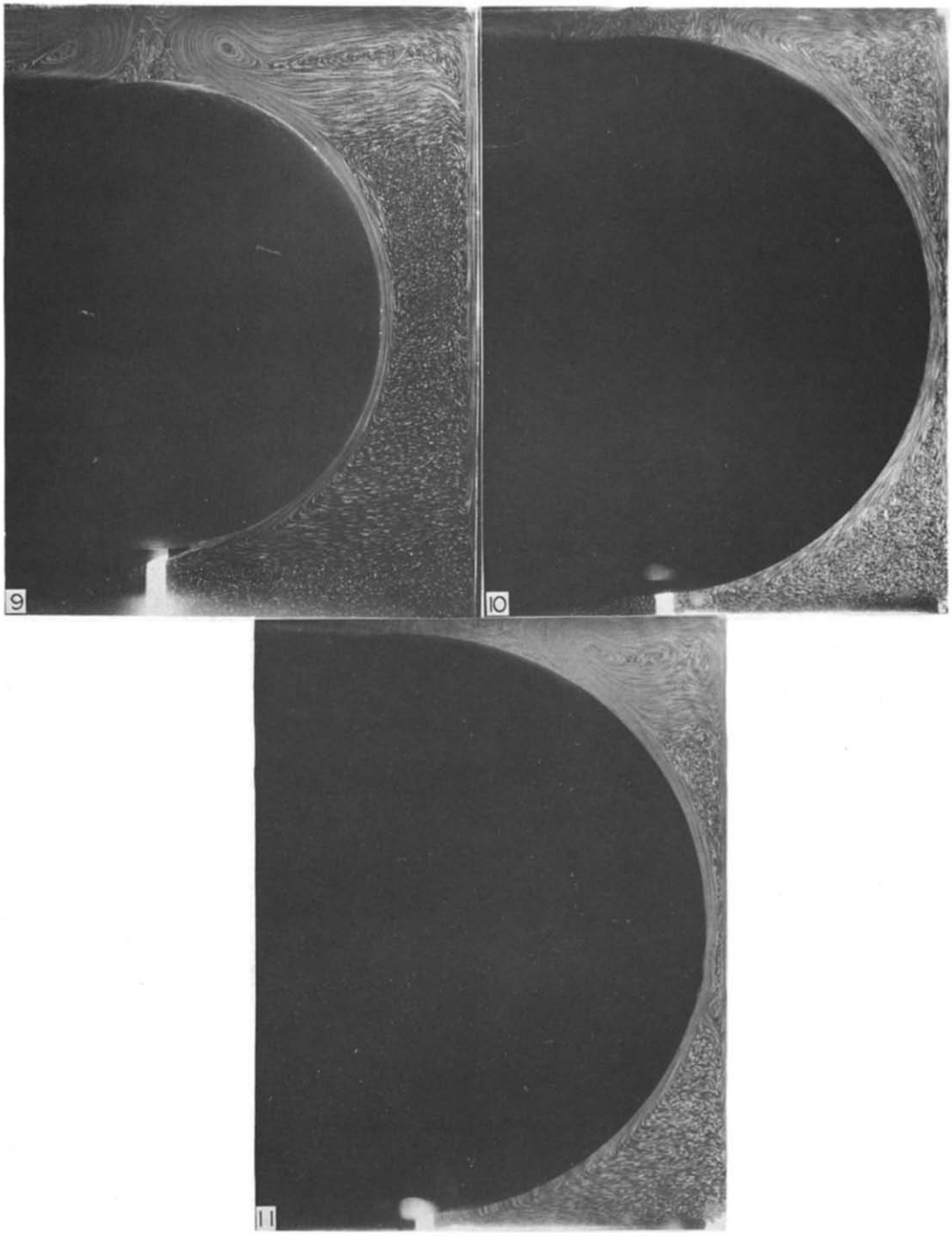

FIG. 9. Random cellular flow for 20 cSt silicone fluid, $R = 1.41$, $Gr = 57\,100$.

FIG. 10. Binary flow for 350 cSt silicone fluid, $R = 1.10$, $Gr = 5$.

FIG. 11. Flow pattern for 20 cSt silicone fluid, $R = 1.10$, $Gr = 1548$.

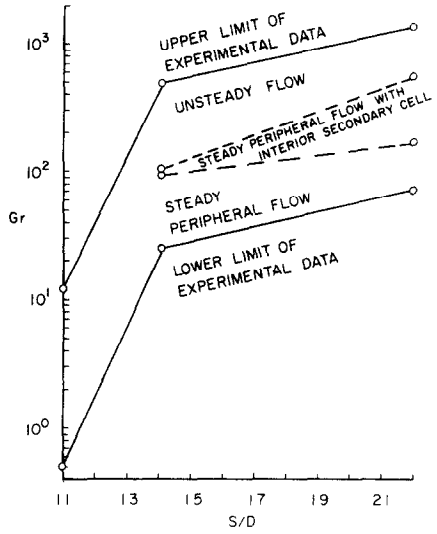

FIG. 12. Range of experimental data and characterization of flow patterns for 350 cSt silicone fluid.

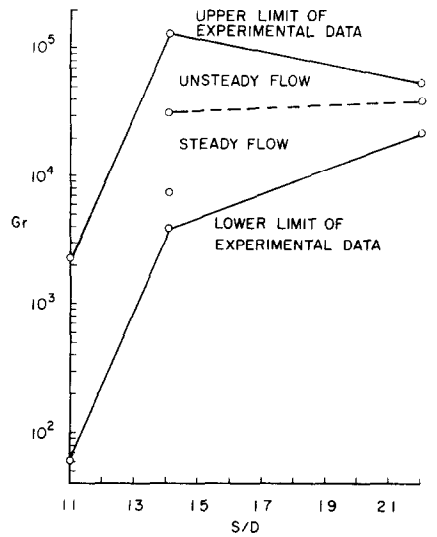

FIG. 13. Range of experimental data and characterization flow patterns for 20 cSt silicone fluid.

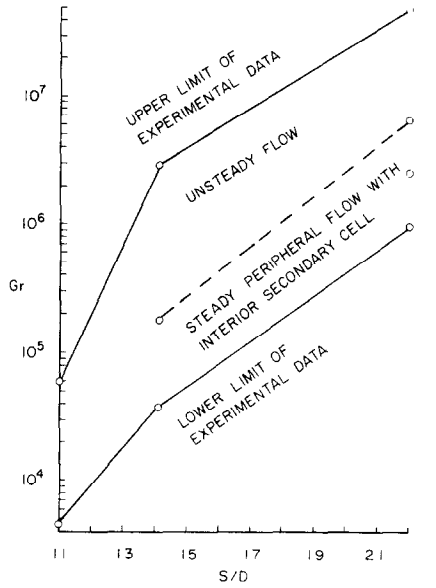

FIG. 14. Range of experimental data and characterization of flow patterns for water.

were observed for 350 cSt silicone oil, 20 cSt silicone oil, and water are presented in Figs. 12, 13 and 14, respectively. Each of these figures indicates the upper and lower limits for the experimental data, as well as the transition point from steady to unsteady flow. Additional steady flow patterns which were observed for intermediate Grashof number ranges are also indicated.

In Fig. 12, it may be observed that the basic steady peripheral flow pattern was observed at low Grashof numbers for the dimension ratio of 2.20 with the 350 cSt silicone fluid. No point of separation of the high-speed fluid layer from the cube side was evident. Secondary cells, located in the neighborhood of the point where the flow over the sphere surface turned into the chimney, first appeared for a Grashof number of approximately 170. These cells remained steady and grew in size until a Grashof number of 560 was reached. Grashof numbers above this value resulted in a very interesting unsteady pattern, the climbing vortices pattern. The flow, which was noted to be periodic and Grashof number dependent, is illustrated in Figs. 6 and 7. A cell formed periodically near the inner body surface at a point located about 20° below the upper vertical axis. Another cell, which was counter-rotating and somewhat removed from the chimney, formed directly above the clockwise rotating cell near the inner body surface, as shown in Fig. 6. After remaining stationary for a short period of time, the lower cell started to climb up the chimney, growing in size and increasing in velocity as it did so. This caused the entire flow field adjacent to the chimney to become rotational, as shown in Fig. 7. Associated with this activity was a very pronounced upward acceleration of fluid in, and adjacent to, the chimney. Moving pictures taken of this pattern clearly indicate this acceleration and also verify that the pattern is symmetric about the upper vertical axis of the inner body. For a Grashof number of 650 the lower cell remained stationary for about 11 s, and the cycle repeated itself at approximately 33 s intervals. For the largest Grashof number investigated, 1390, the cell was stationary for approximately 6 s, and the cycle was repeated every 15–20 s.

For the dimension ratio for 1.41, Fig. 12 shows that the basic steady peripheral flow pattern occurred for Grashof numbers less than 93. No definite point of separation of fluid from the cube wall was observed. It should be noted that the boundary flow was thicker and somewhat slower with the 350 cSt fluid as the gap medium than with either the 20 cSt fluid or water in the gap. For a very small range of Grashof numbers, 93–102, rotating secondary cells were formed adjacent

to the chimney. As shown in Fig. 12, it is expected that such interior secondary cells would not occur for slightly smaller dimension ratios. Grashof numbers above 102 resulted in the unsteady random cellular flow. The separation point for the upward moving fluid over the sphere surface varied from 15° below the upper vertical axis for a Grashof number of 170 to 20° for a Grashof number of 500. Rotating cells, one on each side of the chimney, were observed where the separated flow turned to move across the top of the cube. These cells appeared to form as the primary flow separated, and they dispersed shortly after forming.

For the dimension ratio of 1.10, the flow was unsteady throughout the Grashof number range, even though the minimum Grashof number was much lower than for other dimension ratios. This was typical of all test fluids utilized. For the 350 cSt fluid, the flow was observed to separate from the inner body surface at a point approximately 35° below the upper vertical axis of the sphere. The extreme upper region of the gap was almost stagnant for small Grashof numbers, but flow was induced in this region for Grashof numbers greater than 0.5. As the Grashof number was increased numerous unsteady three-dimensional cells appeared in this area.

For the 20 cSt silicone fluid, Fig. 13 indicates that the transition Grashof number was almost constant for dimension ratios of 1.41 and 2.20. For the dimension ratio of 2.20, the steady peripheral flow with an interior secondary cell occurred for Grashof numbers less than 39 000. For larger Grashof numbers, an unsteady periodic pattern, the climbing vortices flow, occurred. In this pattern, a cell was periodically formed adjacent to the chimney at its base. After formation, the cell remained stationary for a short time then proceeded to move upward along the side of the chimney. As it moved upward, fluid was lost to the central region, and finally the vortex identity disappeared as the cell was engulfed by the high-speed fluid layer along the top of the cube. For a Grashof number of 39 900 these cells would form, rise, and disperse in about 15 s. New cells would form about 10 s after the process had been completed. For the maximum Grashof number of 534 400, the time required for the process to be completed had decreased to about 10 s, and new cells formed almost immediately. For Grashof numbers above approximately 315 700 a weak recirculation flow was also observed in the upper portion of the gap. Fluid from the central region was entrained by the high-speed layer flowing over the surface of the inner body. This resulted in a movement of some of the fluid from the layer flowing down the side of the cubical enclosure toward the sphere.

For the dimension ratio of 1.41, the basic peripheral flow pattern was observed only for Grashof numbers below about 7400. A point of separation was located slightly above a horizontal plane through the bottom of the inner body for the whole range of Grashof numbers investigated, and the area below the separation was filled with essentially stagnant fluid. For Grashof numbers above 7400, the pattern remained steady, but a recirculation motion began in the upper gap region. Incorporated in this recirculation flow were two secondary cells, one adjacent to the chimney and one near the corner of the cubical enclosure. This pattern persisted to a Grashof number of 32 000, and for larger values a random cellular flow occurred. Two small counter rotating cells were first formed on the surface of the inner body near the base of the chimney. The formation of the cells was followed by their upward movement until they were absorbed by the boundary flow across the top. A well-developed flow in the chimney region would then form for a short period, after which the sequence of events just described would again occur. This process was noted to be repeated with a period of approximately 110 s. As the Grashof number was increased, the inner body high-speed flow layer separated from the surface before reaching the upper vertical axis. For a Grashof number of 32 000, separation occurred at about 10° below this axis, and for a Grashof number of 123 100, the separation point had moved to 25° below the axis. For Grashof numbers slightly above 32 000 the portion of the gap where the thermal plume had previously existed was dominated continually by random motion. Slugs of fluid from the boundary flow over the sphere surface were ejected into the upper vertical axis region, and these slugs would rise in an erratic fashion to the top of the enclosure where the fluid was absorbed by the primary flow across the top.

For the dimension ratio of 1.10, unsteady flow was again observed throughout the Grashof number range shown in Fig. 13. This flow was of the basic binary type, with the upper gap region being dominated by unsteady activity characterized by the non-periodic formation of multiple rotating cells. For Grashof numbers above 328, a recirculation flow was noted in the upper central flow region, and this recirculation generated two cells in the primary eddy, similar to those shown in Fig. 4.

For water as the test fluid, Fig. 14 shows the categorization of the flow patterns observed and the range of experimental data. For the two larger dimension ratios, the peripheral flow with interior secondary cells was found to be the basic steady pattern for low Grashof numbers. For the dimension ratio of 2.20, two secondary cells were present in the flow field. One of these cells is located about halfway up the chimney, and the other is near the top of the enclosure. A corner eddy and several small eddies along the side of the cubical-enclosure were also noted. Considerably more motion was observed in the lower region for this case than for silicone oils as test fluids. This flow existed for Grashof numbers up to 6 611 000, at which point a tertiary cell was generated in the upper portion of the gap. The two cells adjacent to the chimney still existed as they did for small Grashof numbers, and a third cell was located near the surface of the inner body. Increasing the Grashof number above 6 611 000 for water as the test fluid resulted in an unsteady pattern in which the upper central region was dominated by three-dimensional activity. This pattern was typical of the unsteady interior flow pattern.

For the dimension ratio of 1.41, the steady peripheral flow with interior secondary cells was observed for Grashof numbers less than about 177600. Larger Grashof numbers resulted in the formation of two counter rotating cells on the sphere surface at the base of the chimney. These small cells circulated in opposite directions in the primary flow on each side of the vertical axis. Also noted at this point was a recirculation of flow in the upper interior region. Several small eddies were located between the primary flow across the top of the cube and the recirculating flow. Further increases in the Grashof number resulted in a widening of the vertical axis region where the counter rotating cells had existed. When a Grashof number of 494000 was reached, the cells no longer appeared, and this portion of the gap was completely dominated by random activity.

The typical unsteady binary type flow was observed throughout the Grashof range for the dimension ratio of 1.10. Very unpredictable, random motion was observed immediately above the inner sphere. For Grashof numbers greater than 24000 a strong recirculation flow in the upper central region developed, and associated with this occurrence was the formation of cells between the primary flow and the recirculating flow. Three-dimensional flow in the upper central portion of the gap also became more apparent as the Grashof number was increased.

Detailed descriptions of the flow patterns which occur due to natural convection in a somewhat complicated, three-dimensional geometry are given in the foregoing paragraphs. These descriptions should enable realistic assumptions to be made regarding flows to be expected in a wide variety of geometries encountered in practice. A note of caution is warranted in using Figs. 12–14 however. In going from a dimension ratio of 2.20 to a dimension ratio of 1.41, drastic changes were not observed in the flow patterns, so interpolation between these dimension ratios could be effected with a reasonable degree of confidence. This is not the case, however, in proceeding from the dimension ratio of 1.41 to the dimension ratio of 1.10. Here there is a complete change in the flow pattern type, so interpolation could be dangerous. It is suspected that the flow pattern observed for the dimension ratio of 1.41 would continue to occur until the minimum spacing between the cube and sphere became such that interference occurs between inner and outer body high-speed flow layers. For smaller dimension ratios, the binary flow would be expected. Detailed information to define this critical dimension ratio is not available, however. Also, it should be kept in mind that, although observations presented here are for a two-dimensional plane of light, the flow patterns must actually be three-dimensional due to the shape of the bounding surfaces. Observation of other cross-sections would likely reveal additional characteristics of the flow field. These results should enable a much better understanding of natural convection flows than is currently available, however. Also, temperature fields to be expected may be inferred from these results.

CONCLUSION

This paper presents the results of an experimental investigation of the flow patterns which occur due to natural convection in a liquid confined between a heated sphere and a cooled surrounding cube. Photographs and written descriptions are given for dimension ratios between 1.10 and 2.20 and for Grashof numbers between 0.5 and 50000000. Liquids utilized were water, 20 cSt silicone oil, and 350 cSt silicone oil, giving an approximate Prandtl number range of 2 to 4500.

Curves are presented which enable the prediction of the type of flow pattern which will occur for the prescribed ranges of the independent variables. It was found that for all the fluids used, the flows could be classified into four steady patterns and four unsteady patterns. Except for the smallest dimension ratio investigated, steady flows always occurred at small Grashof numbers while unsteady flows occurred for large Grashof numbers. For the smallest dimension ratio, interference of the up-flow and down-flow layers occurred, and the flow was unsteady under all conditions.

Representative examples of still photographs are shown; the study also utilized motion picture photography and direct visual observation. Besides being of interest in themselves, these results will be of value in interpreting temperature field measurements in complicated geometries. Not only should the visual work assist in obtaining analytical or numerical solutions, but even if such solutions should prove to be intractable, the visual work will be valuable in the selection of appropriate approximations. It is felt that these results represent a step forward in the understanding of natural convection processes in confined regions of complicated geometry.

Acknowledgement—The investigation described in this paper was supported by the National Science Foundation under Grant No. GK-31908.

REFERENCES

1. L. R. Mack and E. H. Bishop, Natural convection between horizontal concentric cylinders for low Rayleigh numbers, *Q. Jl Mech. Appl. Math.* **21**, 223–241 (1968).
2. P. F. Hodnett, Natural convection between horizontal heated concentric circular cylinders, *J. Appl. Math. Phys.* **24**, 507–516 (1973).
3. L. R. Mack and H. C. Hardee, Natural convection between concentric spheres at low Rayleigh numbers, *Int. J. Heat Mass Transfer* **11**, 387–396 (1968).
4. L. Crawford and R. Lemlich, Natural convection in horizontal concentric cylindrical annuli, *I/EC Fundamentals* **1**, 260–264 (1963).
5. M. R. Abbott, A numerical method for solving the equations of natural convection in a narrow concentric cylindrical annulus with a horizontal axis, *Q. Jl Mech. Appl. Math.* **17**, 471–481 (1964).
6. R. E. Powe, C. T. Carley and S. L. Carruth, A numerical solution for natural convection in cylindrical annuli, *J. Heat Transfer* **93C**(2), 210–220 (1971).
7. E. H. Bishop, L. R. Mack and J. A. Scanlan, Heat transfer by natural convection between concentric spheres, *Int. J. Heat Mass Transfer* **9**, 649–662 (1966).
8. J. A. Scanlan, E. H. Bishop and R. E Powe, Natural convection heat transfer between concentric spheres, *Int. J. Heat Mass Transfer* **13**, 1857–1872 (1970).
9. S. H. Yin, R. E. Powe, J. A. Scanlan and E. H. Bishop,

Natural convection flow patterns in spherical annuli, *Int. J. Heat Mass Transfer* **16**, 1785–1795 (1973).
10. C. Y. Liu, W. K. Mueller and F. Landis, Natural convection heat transfer in long horizontal cylindrical annuli, Paper 117, in *International Developments in Heat Transfer*, Vol. 5, pp. 976–984. A.S.M.E., New York (1961).
11. U. Grigull and W. Hauf, Natural convection in horizontal cylindrical annuli, paper 60, in *Proceedings of the Third International Heat Transfer Conference*, Vol. 2, pp. 182–185. A.I.Ch.E., New York (1966).
12. J. Lis, Experimental investigation of natural convection heat transfer in simple and obstructed horizontal annuli, paper 61, in *Proceedings of the Third International Heat Transfer Conference*, Vol. 2, pp. 196–204 (1966).
13. R. E. Powe, C. T. Carley and E. H. Bishop, Free convection flow patterns in cylindrical annuli, *J. Heat Transfer* **91C**(3), 310–314 (1969).
14. N. Weber, R. E. Powe, E. H. Bishop and J. Scanlan, Heat transfer by natural convection between vertically eccentric spheres, *J. Heat Transfer* **95C**(1), 47–52 (1973).
15. C. T. McCoy, R. E. Powe, E. H. Bishop, N. Weber and J. A. Scanlan, Free convection between a vertical cylinder and a spherical enclosure, *Proceedings of the Fifth International Heat Transfer Conference*, Tokyo. In press.
16. R. E. Powe, S. H. Yin, J. A. Scanlan and E. H. Bishop, A technique for visualization of the very slow motion of water in enclosed spaces, *J. Heat Transfer* **95C**(3) (1973).
17. J. W. Elder, Laminar free convection in a vertical slot, *J. Fluid Mechanics* **23**(1), 77–98 (1965).
18. J. W. Elder, Numerical experiments with free convection in a vertical slot, *J. Fluid Mech.* **24**(4), 823–843 (1966).
19. A. Watson, The effect of the inversion temperature on the convection of water in an enclosed rectangular cavity, *Q. Jl Mech. Appl. Math.* **25**(4), 423–446 (1972).

CONVECTION NATURELLE DANS LES LIQUIDES ENTRE UNE SPHERE ET UNE ENCEINTE CUBIQUE

Résumé—On présente les résultats de la visualisation de la convection naturelle dans des liquides placés entre une sphère chauffée et son enceinte cubique et froide. Trois sphères différentes sont utilisées avec un cube de 25,15 cm d'arête, pour obtenir des rapports dimensionnels (rapport de la longueur de l'arête au diamètre de la sphère) allant de 1,10 à 2,20 et avec des nombres de Grashof depuis 0,5 jusqu'à 50 000 000. On présente la description détaillée des configurations d'écoulement, description appuyée par des photographies. Les fluides utilisés sont l'eau, et l'huile de silicone à 20 cS et 350 cS. Il est possible de classer les configurations, pour ces fluides et toutes ces géométries, en quatre figures stables et quatre autres instables. Sauf pour le plus petit rapport dimensionnel 1,10, les écoulements stables concernent les petits nombres de Grashof, tandis que les écoulements instables se rencontrent aux nombres élevés. On note une interférence entre les couches ascendante et descendante pour le plus petit rapport dimensionnel et ceci provoque une configuration unique.

STRÖMUNGSUNTERSUCHUNGEN BEI NATÜRLICHER KONVEKTION VON FLÜSSIGKEITEN ZWISCHEN EINER KUGEL UND IHREN KUBISCHEN UMSCHLIESSUNGSWÄNDEN

Zusammenfassung—Die Arbeit berichtet über eine Untersuchung zur Sichtbarmachung der natürlichen Konvektion von Flüssigkeiten im Raum zwischen einer beheizten Kugel und ihren gekühlten, kubischen Umfassungswänden. Es wurden drei verschiedene Kugeln verwendet; sie befanden sich in einem kubischen Behälter mit der Seitenlänge von 25,15 cm; das Längenverhältnis (Seitenlänge des Kubus zum Kugeldurchmesser) wurde von 1,10 bis 2,20, die Grashof–Zahl von 0,5 bis 50 000 000 variiert. Die Strömungsformen werden mit Hilfe von Photographien eingehend beschrieben. Als Versuchsflüssigkeiten wurden Wasser, Silikonöl mit 20 cS sowie mit 350 cS verwendet. Für alle diese Flüssigkeiten und Geometrien konnten die Strömungsformen in 4 stationäre und 4 instationäre Gruppen eingeteilt werden. Mit einer Ausnahme für das kleinste Längenverhältnis von 1,10 traten stationäre Strömungen immer bei kleinen Grashof–Zahlen auf, während instationäre Strömungen bei großen Grashof–Zahlen auftraten. Eine gegenseitige Beeinflussung zwischen auf- und abwärtsströmenden Schichten wurde beim kleinsten Längenverhältnis beobachtet und führte zu ziemlich einzigartigen Strömungsformen.

ИЗУЧЕНИЕ СТРУКТУРЫ КОНВЕКТИВНОГО ДВИЖЕНИЯ В ЖИДКОСТЯХ МЕЖДУ КУБОМ И СОДЕРЖАЩЕЙСЯ В НЕМ СФЕРОЙ

Аннотация — Приводятся результаты визуального исследования свободного конвективного течения в жидкостях, находящихся между нагретой сферой и охлажденным кубическим объемом. Использовались три различные сферы. Сторона куба равнялась 25,15 см. Геометрический параметр (отношение длины стороны куба к диаметру сферы) изменялся от 1,10 до 2,20, при числах Грасгофа от 0,5 до 50 000 000. Приводится подробное описание режимов течения, иллюстрированное фотографиями потока. В качестве жидкостей использовались вода, 20 сст силиконовое масло и 350 сст силиконовое масло. Течения всех жидкостей и их геометрии могут быть описаны четырьмя стационарными и четырьмя нестационарными режимами. За исключением случая с наименьшим отношениям размеров 1,10, стационарные течения всегда имели место при небольших числах Грасгофа, тогда как нестационарные — при больших числах Грасгофа. При наименьшем отношении размеров отмечалось взаимодействие слоев восходящего и нисходящего потоков, что создавало довольно специфическую картину течения.